

3.11 Quantum magnetic radius of the electron

The quantum features of the electron define its preferential velocities (energies), referred also as quantum velocities. Electron motions with such velocities exist not only in the Hydrogen atoms, but in all atoms. In Hydrogen they appear explicitly, as the lowest level energy of the series. In other atoms, however, they does not appear explicitly, because their energy levels are added with the IG potential of the atomic structure. These potentials are included in the CL space pumping and photon emission. The electron motion, with quantum velocities however is involved in all emission and absorption spectral lines. For this reason we will pay a special attention about the quantum conditions corresponding to suboptimal velocities (electron energies below 13.6 eV).

There is one value of the electron radius, that fits well the spectroscopic data, according to the quantum mechanics. This is the Quantum Mechanical radius R_{QM} . It is related to the Compton radius by the factor of $\sqrt{3}$

$$R_{QM} = \sqrt{3}R_c = 1.732R_c \quad (3.24)$$

In the following analysis we will derive the equivalent quantum radius of the electron. This is the radius, corresponding to the equivalent radial field, shown in Fig. 3.6. It is evident, that this radius depends of the subharmonic number.

Let to derive, in first, the equivalent radius for the first harmonic, corresponding to energy of 13.6 eV.

A. Case: Quantum radius at first harmonic (at optimal confined velocity $v = \alpha c$):

In CL space with normal ZPE (not superconducting state) the quantum magnetic field Φ_o is given by the relation

$$\Phi_o = \frac{h}{q_o} = 4.135 \times 10^{-15} \quad Wb \quad (3.25)$$

The quantum magnetic strength H_o is:

$$H_o = \frac{B_o}{\mu_o} = \frac{\Phi_o}{\mu_o S} = \frac{h}{q_o \mu_o S} \quad \frac{A}{m} \quad (3.26)$$

where: B_o is the quantum magnetic inductance,
 μ_o is the permeability of free space (cosmic lattice),

S is the surface area for which the magnetic flux flows.

From the field configuration of the electron at optimal confined velocity discussed in §3.4 and illustrated in Fig. 3.5 and 3.8, becomes evident, that the only surface that may satisfy the definition is the boundary surface. At accepted ratio $k_{hb} = R_{mb}/R_c = 4$, the shape of surface for the first harmonic is slightly oblate spheroid. For the second and next subharmonics, the shape approaches a sphere. In a first approximation we may accept, that the surface has a spherical shape also for the first harmonic motion. Then substituting $S = 4\pi(k_{hb}R_c)^2$ in Eq. (3.26) we get.

$$H_o = \frac{h}{q_o \mu_o 4\pi(k_{hb}R_c)^2} \left[\frac{A}{m} \right] \quad (2.27)$$

The Eq. (3.27) having dimensions of [A/m], can be regarded as a quantum magnetic strength.

The magnetic moment of the electron was given by Eq. (3.23). It has dimensions [Am²]. The electrical field of the screwing electron generates disturbance in the CL space as magnetic field. The disturbance volume is obviously external to the helical structure, having a similar shape but with $r_{eq} > r_e$. Due to the larger R/s_e ratio, we can express the volume of the electron structure as a torus volume with larger radius r_{eq} and smaller one r_e . $V_{eq} = 2\pi^2 R_c (r_{eq}^2 - r_e^2)$ Then dividing the magnetic moment on that volume, we will obtain expression with the same dimensions [A/m].

$$\frac{\mu_e}{V_{eq}} = \frac{q_o h}{4\pi m_e 2\pi^2 R_c (r_{eq}^2 - r_e^2)} \left(1 + \frac{\alpha}{2\pi} \right) \quad [A/m] \quad (3.28)$$

The Eq. (3.28) has a same dimensions as (3.27), and expresses also the quantum magnetic strength H_o .

Equating (3.27) and (3.28) and solving for r_{eq} , we get the quantum equivalent radius for the first harmonic.

$$r_{qe} = \left[\frac{q^2 \mu_o R_c k_{hb}^2}{2\pi^2 m_e} \left(1 + \frac{\alpha}{2\pi} \right) + r_e^2 \right]^{1/2} \quad (3.29)$$

For $k_{hb} = 4$, we have ($r_{qe} = 1.057 \times 10^{-13}$) m .

The equivalent quantum field is a torus with a same radius R_c but $r_{eq} > r_e$. The real equivalent quantum radius then is:

$$R_{eq} = R_c + r_{eq} \quad (3.30)$$

B case: Quantum radii at subharmonic numbers $1 \leq n \leq 3$.

In a subharmonic motion, the flux Φ_o is the same but B is changed because boundary surface s is larger. The boundary radius at n subharmonic is: $R_{mb}(n) = nR_c k_{hb}$. Then the boundary surface is:

$$S(n) = 4\pi(nR_c k_{hb})^2$$

Substituting the expression of $S(n)$ in (3.26) and processing in a similar way as the previous case, we get the equivalent radius in function of the subharmonic number n .

$$r_{qe}(n) = \left[\frac{q^2 \mu_o n^2 R_c^2 k_{hb}^2}{2\pi^2 m_e} \left(1 + \frac{\alpha}{2\pi} \right) + r_e^2 \right]^{1/2} \quad (3.31)$$

The quantum radius is always smaller, than the boundary radius. It could be considered as an equivalent radius for idealised E-field with square shape. For this reason it is convenient for calculations related with energy.

The values of the equivalent radius r_{qe} , the boundary radius R_{mb} , and the relevant energy for few subharmonics are shown in Table 3.3.

Table 3.3

n	E [eV]	r_{eq} [m]	$R_{mb}(n)$ [m]	$(R_c + r_{eq})/R_c$
1	13.6	1.057E-13	1.544E-12	1.273
2	3.401	2.1087E-13	3.089E-12	1.546
3	1.51	3.161E-13	4.634E-12	1.818
4		4.215E-13		

In the derivation of Eq. (3.31) we have assumed, that the equivalent radius is symmetrical around the radius R_c . Then the condition $r_{eq} \leq R_c$ must be satisfied. From Table 3.3 we see, that this condition is satisfied up to the third subharmonic. The fourth subharmonic does not satisfies this condition, so the Eq. (3.31) is valid for the for $1 \leq n \leq 3$ only. **For these cases, the equivalent quantum radius is still equal to $(R_c + r_{eq})$.**

The last column of Table 3.3 shows the ratio between calculated equivalent quantum radius and the radius R_{QM} , used in the quantum mechanics. The Eq. (3.24) gives the ratio $R_{QM}/R_c = 1.732$. We see that this value is the second and third subharmonic. They correspond to the Balmer and Pashen series in Hydrogen. In Chapter... we will see, that the electron motion in the most available series in all atoms is similar as the motion of the Balmer and Pashen series. Then the calculated equivalent quan-

tum radius appears consistent with the spectral data.

C case: Quantum radii at subharmonic numbers $n > 3$.

For subharmonics larger than 3, the equivalent quantum field will not have the same radius R_c , but larger, as shown in Fig. 3.17.

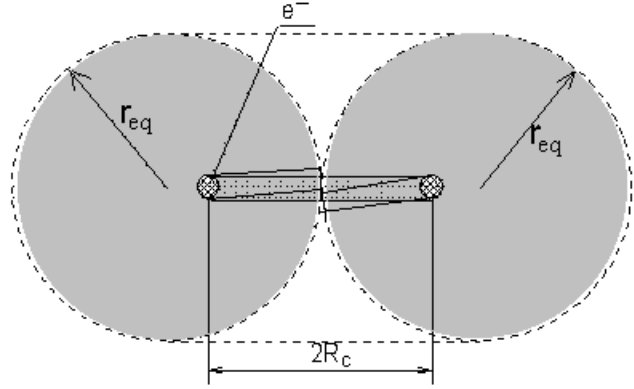


Fig. 3.17

Equivalent quantum radius of the electron for subharmonics numbers > 3 .

In this case the volume V can be expressed as: $V_{eq} = 2\pi^2(r_{eq}^3 - R_c r_e^2)$. Neglecting the helical factor $\alpha/2\pi$, the derived radius r_{eq} in this case is:

$$r_{eq}(n) = \left[\frac{q^2 \mu_o n^2 R_c^2 k_{hb}^2}{2\pi^2 m_e} + R_c r_e^2 \right]^{1/3} \quad (3.32)$$

The equivalent quantum radius is:

$$R_{eq} = 2r_{eq} \quad \text{for } n > 3 \quad (3.33)$$

Table 3.4 shows the equivalent and boundary radii for subharmonics numbers $n > 3$.

Table 3.4

n	E [eV]	r_{eq} [m]	$R_{eq}(n)$ [m]	$R_{mb}(n)$ [m]
4	0.85	4.092E-13	8.184E-13	6.178E-12
5	0.544	4.748E-13	9.496E-13	7.72E-12
6	0.377	5.361E-13	1.072E-12	9.268E-12

We see that at smaller velocity the quantum radius is larger. The velocity for the sixth subharmonic is 3.646E5 m/sec. (see Table 3.1). The electron motion around the proton is characterized with large velocities. The motion of free electrons in metals however is characterised with small velocities.

It is interesting to derive the electron equivalent quantum radius at small velocity, because, it will help to unveil the interaction effect with the at-

oms. This interaction plays important role in understanding the resistivity of the conductors.

D. Case: Equivalent quantum radius of the electron at small velocity

The average electron velocity in copper according to the drift theory is 3.54E-05 m/sec. This is much smaller, than the sixth subharmonic velocity. Obviously the expected equivalent radius will have much larger value. In such conditions, the volume of the electron structure become insignificant and we can ignore it. The configuration of the E-field lines in very small velocity is also change. The density of the terminated lines at the boundary conditions becomes more uniform. The helicity however is preserved. Having in mind all this considerations, we may accept that the E-field occupy a spherical volume. Then the energetic equivalent volume is expressed by $V_{eq} = \frac{4}{3}\pi R_{eq}^3$ (3.34)

The contribution from the term $\alpha/2\pi$ will be neglected for simplicity.

We can not apply a similar approach for calculation of R_{eq} as the previous cases, because, the boundary conditions for large volume does not work. Instead of that, we will consider the change of the magnetic flux Φ due to the slower electron rotation in comparison to its rotation at first harmonic. Consequently, now we will reference the magnetic flux surface S to the surface corresponding to the equivalent quantum radius at first harmonic.

$$S = 4\pi^2 R_c r_{eq1}$$

where: $r_{eq1} = 1.057 \times 10^{-13}$ is the equivalent radius for a first harmonic motion

In a small velocity case, the rotating speed of the electron will be smaller, but the fundamental period is unchanged. Let to assume that the positron makes n cycles for a full electron turn. Then the n dependence of velocity v according to Eq. (3.16) is:

$$n = \frac{\alpha c}{v} \quad (3.35)$$

The lattice twisting will be n times smaller, and so the magnetic flux also:

$$\Phi = \frac{h}{nq} \quad (3.36)$$

The magnetic strength then is:

$$H = \frac{\Phi}{\mu_o S} = \frac{h v}{\alpha c q \mu_o 4\pi^2 R_c r_{eq1}} \quad (3.37)$$

The volume expressed by Eq. (3.34) is the equivalent volume for the quantum interaction. Dividing the magnetic moment by this volume, we get:

$$\frac{\mu_e}{V_{eq}} = \frac{qh}{4\pi m_e \frac{4}{3}\pi R_{eq}^3} = H \quad (3.38)$$

Solving (3.37) and (3.38) for R_{eq} , we get the equivalent quantum radius in function of the velocity (for $v \ll \alpha c$).

$$r_m = \left[\frac{3\alpha c q^2 \mu_o R_c r_{eq1}}{4\pi m_e v} \right]^{1/3} \quad (3.39)$$

The graphical plot of Eq. (3.39) for velocity range between 10^{-6} m and 1 m is shown in Fig. 3.18, where the velocity is in a log scale.

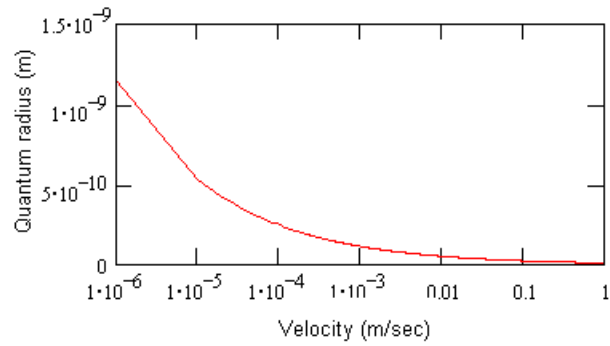


Fig. 3.18

Quantum radius of the electron for low velocities

The graphical plot of Eq. (3.39) shows significant increase of the magnetic radius at very low velocity. Such velocities exist in the metal conductors.

Example: The average electron velocity in copper according to the drift theory is 3.54E-05 m/sec. Then the corresponding magnetic radius according to Eq. (3.39) is 2.77E-10 m. This is comparable to the gaps between the atoms. The magnetic field of the moving electron, obviously interact with the protons fields. This could explain the ohmic resistance. The existing so far classical theories failed to explain the ohmic resistance in metals. The quantum mechanics gives explanation by the wavefunctions, but fails to give a clear classical explanation.

The quantum radius for small velocities, can be expressed also by the electron kinetic energy.

For this purpose, the velocity in Eq. (3.39) can be substituted by the expression (3.40), where, the energy is in eV.

$$v = \sqrt{\frac{2E_{ev}q}{m_e}} \quad (3.40)$$

The equivalent quantum radius in function of the kinetic energy is:

$$R_{eq} = \left[\frac{3\alpha c \mu_o R_c r_{eq} \sqrt{q}}{4h\sqrt{2E_{ev}m_e}} \right]^{1/3} \quad \text{for } E_{ev} \ll 1.36 \text{ eV} \quad (3.41)$$

where: E_{ev} - is the electron kinetic energy in (eV).

The quantum radius dependence of the velocity is very important feature of the moving electron. From one hand it helps to analyse the orbital motion conditions in the atoms. In this aspect, the equations (3.29) and (3.31) are relevant. From the other hand, the quantum radius helps to understand the interaction of the free electrons in the metals with the atomic nuclei of the metallic crystal. In this case the equations (3.39) and (3.41) are relevant.

We may summarize the analysis in the following conclusions:

- **At optimal confine velocity corresponding to energy of 13.6 eV, the transverse equivalent quantum radius is smallest.**
- **The dependence of the electron quantum radius from the velocity helps to understand the orbital motion of the electron around the proton and the ohmic resistance in the metals.**

3.11.A Relativistic motion of the electron. Relativistic gamma factor and quantum efficiency.

So far the quantum motion of the electron for optimal and suboptimal velocity was discussed. The electron motion with velocities larger than optimal one also exhibit a quantum feature, but the quantum effect is weaker. For the correct physical analysis of the electron behaviour, two relativistic factors are necessary to be considered: the relativistic gamma factor and the quantum efficiency. The first one is well known from the relativistic theory. The second one is not considered so far, but it is very important for the correct estimation of the

electron behaviour. It directly reflect also to the behaviour of the relativistic muon. In the present paragraph, both factors are derived.

According to basic postulates in the special relativity, the Lorentz transformation is used, where the gamma factor is given by

$$\gamma = (1 - v^2/c^2)^{-1/2} \quad (3.42.A)$$

In the next paragraph the same gamma factor will be derived based on the electron motion behaviour.

3.11.A.1 Quantum efficiency

(A) Quantum efficiency at suboptimal velocity

The quantum effect in this case is strong, so it is enough to derive expressions in function of subharmonic number.

Quantum efficiency dependence from the boundary conditions

The surface of the boundary conditions is proportional to the magnetic radius, and latter to the subharmonic number. The smallest boundary surface corresponds to the first harmonics whose quantum efficiency is a maximum. Consequently $\eta_{BC} = 1/n$, where n is the subharmonic number.

Quantum efficiency dependence from the hummer drill effect

This problem is discussed in Chapter 4 in relation with the Fractional quantum Hall experiments. It is shown that the efficiency is inverse proportional to the subharmonic number.

$$\eta_{HD} = 1/n$$

The total quantum efficiency is a product of both type efficiencies. This is **the quantum efficiency for suboptimal velocity motion.**

$$\eta = 1/n^2 \quad (3.42.B)$$

The quantum efficiency affects the line width. Then comparing the linewidths (normalized to the wavelength) from the different series of the Hydrogen atom, we may test the validity of Eq. (3.41.a). The Lyman series should contain the narrowest lines.

(B) Quantum efficiency at superoptimal velocity, (velocity above the optimal one but lower, than the relativistic velocities)

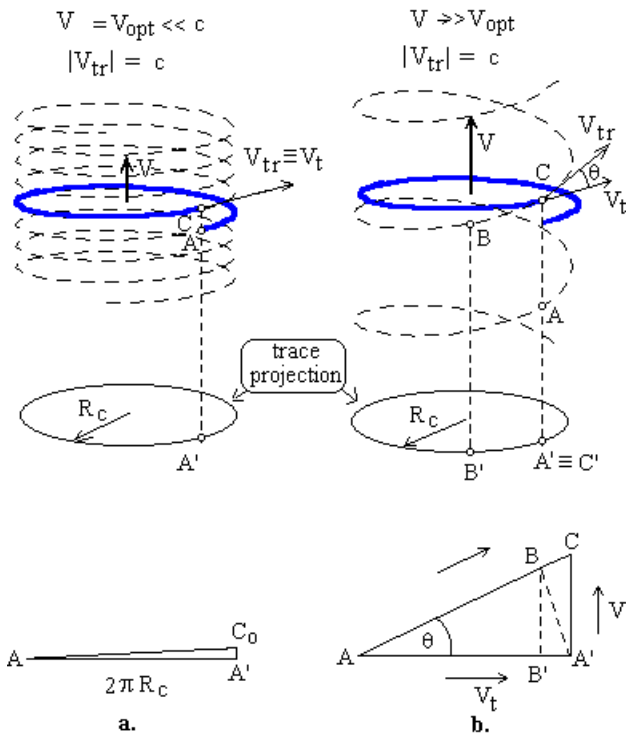
In this case the quantum efficiency is determined by the efficiency of the hummer-drill effect. The analysis in this case is similar as the hummer-

drill effect analysis in the Quantum fractional Hall effect, discussed in Chapter 4.

(C) Quantum efficiency at relativistic velocities.

The decreased efficiency in its case is related with the large cosine between the vector of trace velocity and the vector of the electron-positron oscillation.

Fig. 3.18.A shows the confined electron motion for both cases: a. - for optimal velocity and b. - for superoptimal one. The front end traces are shown by dash line, while the electron shape with thick blue line. The trace projection on a plane normal to the axial velocity V is a circle, shown below the helical trace. The selected points from the trace are denoted in the circle projection with the same letters with primes (').



3.18.A

Electron motion with optimal (a.) and superoptimal (b.) velocity

We will consider the two times:

τ_c - the motion cycle time; T is the period of one full electron system rotation.

t_c - the proper frequency time, equal to the Compton time

This two times determine two different properties:

- **The cycle time determines the wavelength of the generating wave (also the magnetic radius) - the magnetic interaction with CL space**
- **The proper frequency time determines the quantum interaction with the CL space (interaction with the SPM vector by the hummer-drill effect)**

Let to make the **assumption, that the proper frequency of the electron-positron system is unchanged**, $t_c = 1/\nu_c = const$, i. e. it does not depend of the axial velocity. If p. A is our initial reference point, the electron system will complete one full proper cycle in p. B, earlier than the completion of the motion cycle time in p. C.

It is convenient to unfold the trace motion, as shown in the bottom of the Fig. 5.18A for both cases. In this way the proportional distances between the points and the angles between the velocity vectors are preserved. They are given in a table form below.

	AA'	AC	AB	A'C
paths:	$2\pi R_c$	cT_c	$2\pi R_c$	VT_c
velocity:	$2\pi R_c/T_c$	c	$2\pi R_c/T_c$	V

We see that:

For case **a.** the direction of the trace velocity V_{tr} coincides with the direction of the oscillation velocity vector V_t , while for case **b.** they are crossed by angle θ . In the first case the quantum interaction is optimal, while in the second one it is reduced. Accepting the efficiency at optimal velocity as unity, the efficiency in the second case could be expressed as a ratio of AA'/AB' . This is equal to the ratio of AB/AC . Having in mind, that $AB = AA'$, the quantum efficiency become

$$\eta = \frac{AA'}{AC} = \cos\theta$$

From the timing ratio, we have also:

$$\frac{t_c}{T_c} = \frac{AB}{AC} = \frac{AA'}{AC} = \cos\theta$$

From the unfolded trace we have:

$$AA' = 2\pi R_c, \text{ and} \quad AC = \sqrt{4\pi^2 R_c^2 + V^2 T_c^2}.$$

Substituting and eliminating all parameters but V and c we arrived to the final equation for the quantum efficiency for relativistic velocities.

$$\eta = (1 - V^2/c^2)^{1/2} \quad (42.D)$$

The plot of the quantum efficiency is shown in Fig. 3.18.B.

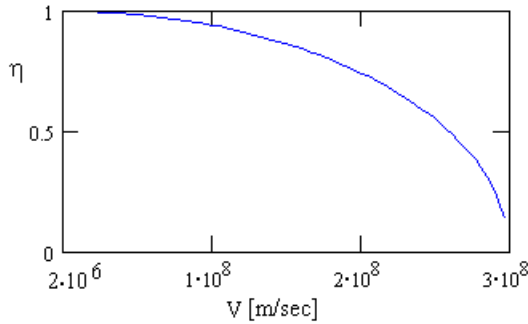


Fig. 3.18.B

Quantum efficiency of the electron motion at relativistic velocities

From the point of view of the physical explanation, the trend of the quantum efficiency is quite reasonable. We see that it appears as inverse function of the relativistic gamma factor.

3.11.A.2 Relativistic gamma factor

According to the special relativity, the gamma factor is equal to the ratio between the relativistic and the nonrelativistic momentum: $\gamma = p_{rel}/p$. It is also equal to the ratio between the relativistic and not relativistic time: $\gamma = T_{rel}/T$.

According to the physical analysis of the electron motion in the previous paragraph, the corresponding two time periods are: $T = t_c$ and $T_{rel} = T_c$. Then the gamma factor is

$$\gamma = \frac{T_c}{t_c} = \frac{1}{\cos\theta} = \frac{1}{\eta} \quad (3.42.E)$$

When expressed by c and V , the gamma factor is:

$$\gamma = (1 - V^2/c^2)^{-1/2} \quad (3.42.F)$$

Conclusion: The relativistic gamma factor and the quantum efficiency are inverse functions. This should be taken into account, when estimating the physical properties of the real particles with

short lifetime. Some processes may obtain quite different physical explanation. This is valid in full for the muon lifetime, for example, leading to a different explanation of the factors that influence its decay

3.12 Quantum loops and orbits

So far we analysed the quantum motion of the electron system in open trajectory. This does not exhaust all the possibility of the electron quantum motion. One special case still exists. This is the quantum motion of the electron in a closed loop. The term quantum loop is more universal, meaning a closed trajectory. A typical case is the electron - positron oscillation trajectories. The term quantum orbit is more suitable for the electron motion around the proton. In this case the proton can serve as a frame of reference, because of its large mass.

3.12.1 Quantum loop conditions

Now we will analyse the motion of a normal electron system, from a point of view of a stationary frame. When performing quantum motion as repeatable loops some portion of the electron orbit may have equipotential paths. The magnetic field created by this motion also could tend to extend the length of these paths. In this conditions the electron - positron system oscillates with small amplitudes. Then we have the following proper frequencies:

$$v_{ep} = v_c \text{ - proper frequency of electron - positron} \quad (3.43.a)$$

$$v_{pc} = 3v_c \text{ - proper frequency of the positron - core} \quad (3.43.b)$$

Let consider two cases of motion:

- very slow motion approaching zero velocity
- motion corresponding to energies from 0.3 to 13.6 eV

In the first case the velocity of both ends of the positron are equal and symmetrical in respect to the stationary CL nodes.

In the second case the velocities of both ends of the positron, are not symmetrical in respect to the stationary CL nodes.

If trying to reference the period of the v_{pc} oscillations to the stationary nodes we will find the following features:

a) the electron system is displaced axially due to the second order helicity by distance equal to the step s_e .

b) the internal positron system is carried by the electron shell

c) the path that the positron system is carried depends of the velocity of the electron shell

If we compare the feature a) with the boundary conditions of MQs, we will see, that: The displacement due to the step s_e does not have a symmetrical counterpart in the boundary conditions. **Consequently it will cause a phase difference between the proper frequency of the electron-positron system and the SPM frequency of the stationary CL nodes.**

Let us estimate this phase delay for electron motion with optimal confined velocity ($E = 13.6$ eV). For this purpose we will present the single coil of the electron as unfold helix, shown in Fig. 3.19.

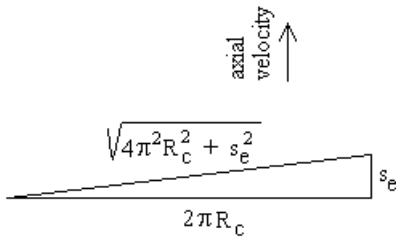


Fig. 3.19

The electron as unfold single coil helix

The hypotenuse of the triangle can be regarded as a path of the front edge of the electron, while the kathet s_e is its axial displacement. If s_e approaches zero, the discrepancy between the oscillations with the proper frequency and the CL node oscillations will disappear. The both frequencies are equal to the Compton frequency. For some finite velocity in the range $0 < v \leq \alpha c$, the phase difference from the discrepancy should be proportional to s_e . We need to reference the phase difference to the full revolution. Then it could be expressed as a ratio between the kathet s_e and the hypotenuse (the other option - the ratio between the two kathets does not provide consistent result later). So the fractional phase difference is:

$$\frac{\Delta\phi}{2\pi} = \frac{s_e}{\sqrt{4\pi^2 R_c^2 + s_e^2}} = 7.2973531 \times 10^{-3} = \alpha \quad (3.43.c)$$

The fractional phase difference, defined in such way appears equal to the fine structure constant. We can refer to it as a **phase difference per one turn.**

The definition of the quantum loop is the following:

The quantum loop is a closed loop trajectory, whose length corresponds to a whole number of carrier oscillations.

Under therm carrier we understand the whole oscillating system containing two proper frequencies,

Let take into account only the discrete velocity values of the system, corresponding to the quantum motion. These velocities are defined by the subharmonic number. The triangle shown in Fig. 3.19 could be considered as a path of the front edge of the electron. At first harmonic (subharmonic) it has the same dimensions, as shown in Fig. 3.19. At any other subharmonic the triangle is similar, but with sides divided to the subharmonic number. Then the phase difference given by Eq. (3.43.c) appears not for one turn of the electron system, but for one proper cycle. Then for a quantum motion at n subharmonic, the phase difference accumulated per one turn of the electron system is:

$$\frac{\Delta\phi}{2\pi}(n) = n\alpha \quad (3.43.d)$$

3.12.2 Quantum loops and orbits for electron with optimal confined velocity. Embedded signature of fine structure constant.

Let us find the path length at which the quantum loop condition for the electron system is fulfilled. The electron system possesses two proper frequencies and we must check the quantum loop condition for both of them. It is reasonable to look for path length defined by some CL space parameter. One of this parameter is the Compton wavelength $\lambda_c = \lambda_{SPM}$. If an electron possessing a first harmonic velocity travels in a closed loop with length λ_c , the number of turns N_T is:

$$N_T = \lambda_c / s_e = 137.03234 \quad (3.43.d)$$

The value of N_T could be regarded as a condition for a phase repetition for two consecutive passages through a chosen point in the loop, keeping in mind a confined (screw-like) motion of the

electron. The trace length of $\lambda_c = 2.4263 \times 10^{-12}$ (m), however, is quite small, when comparing to the Bohr orbit length of $2\pi a_0 = 3.3249187 \times 10^{-10}$ (m). Therefore, we may look for a phase repetition conditions at a larger loop length. From Eq. (3.43.d) we see that N_T is close to $1/\alpha = 137.036$ and this seems not occasional. Then we may substitute N_T in Eq. (3.43.d) by $1/\alpha$ and multiply the expression by λ_c . The latter is a CL space parameter, from one side (a distance that the SPM phase propagates for one SPM cycle) and from the other - the circumference length of the electron structure. In such case we obtain:

$$N_T \lambda_c \approx \frac{1}{\alpha} \lambda_c = 3.24918460 \times 10^{-10} \quad (3.43.e)$$

We see that the obtained value of Eq. (3.43.e) having dimensions of length is equal to the Bohr orbit length given by CODATA 98 up to the 9th significant digit.

$$a_0 = 3.24918460 \times 10^{-10} \quad (\text{m}) \quad (3.43.f)$$

where: $a_0 = 0.52917721 \times 10^{-10}$ (m) - is the radius of the Bohr atomic model of hydrogen.

The term λ_c/α of the expression (3.43.e) is not something new. The important fact, however, is the way of its derivation related with the suggested physical model of the electron. The obtained loop length appears equal to the orbit length of the Bohr atom, defined by the Bohr atomic radius, a_0 . The latter is one of the basic parameters used in Quantum mechanics. From the BSM point of view, however, the physical meaning of this parameter appears different.

According to BSM concept, the well known parameter a_0 used as a radius in the Bohr model, appears defined only by the quantum motion conditions of the electron moving in a closed loop with an optimal confined velocity corresponding to an electron energy of 13.6 eV. Then the main characteristic parameter of the quantum loop is not its shape, but its length.

The identity of Equations (3.43.e) and (3.43.f) also indicates that **the signature of the fine structure constant is embedded in the quantum loop.**

Now we may use the new obtained meaning about the quantum loop associated with the Bohr orbit, and more specifically the orbital length $2\pi a_0$.

For a motion with an optimal confined velocity, the number of electron turns in the quantum orbit is equal to the orbital length divided by the helix step (s_e).

$$\frac{2\pi a_0}{s_e} = \frac{\lambda_c}{\alpha s_e} = 18778.365 \quad (\text{turns}) \quad (3.43.g)$$

Let find at what number of complete orbital cycles (for orbit length of $2\pi a_0$) the phase repetition of the first and second proper frequencies of the electron is satisfied (in other words the smallest number of orbital cycles containing whole number of two frequency cycles). The analysis of the confined motion of the electron in Chapter 3 and 4 of BSM indicates that its secondary proper frequency is three times higher than the first one (the first one is equal to the Compton frequency). Equation (3.43.g) shows that the residual number of first proper frequency cycles is close to 1/3. If assuming that it is exactly 1/3 (due to a not very accurate determination of the involved physical parameters), then the condition for phase repetition of both frequency cycles will be met for three orbital cycles. The whole number of turns then should be $(3\lambda_c)/(\alpha s_e)$. Substituting s_e by its expression given by Eq. (3.13.b) and knowing that $v_e/c = \lambda_c$ we get

$$\frac{3(1-\alpha^2)^{1/2}}{\alpha^2} \quad (\text{turns}) \quad (a)$$

We have ignored so far the relativistic correction, but for accurate estimation it should be taken into account. The relativistic gamma factor for the electron velocity of $v_{ax} = \alpha c$ is $\gamma = (1-\alpha^2)^{-1/2}$. Multiplying the above expression by the obtained gamma factor we get.

$$3/\alpha^2 = \text{integer} \quad (\text{turns}) \quad (b)$$

The validity of obtained expression (a) and (b) could be tested by the following simple procedure: calculating these expressions by using the best experimental value of α , rounding the result to the closer integer (satisfying the condition for two consecutive phase repetitions) and recalculat-

ing the corresponding value of α . The rounded integer (a whole number of turns) could be correct only if the recalculated value is in the range of the accuracy of the experimentally determined α . Let using the recommended value of experimentally measured α according to CODATA 98.

$$\alpha = 7.2973525(27) \times 10^{-3} \quad (\text{CODATA98})$$

where, the uncertainty error is denoted by the digits in the brackets.

The calculated values of α from Eq. (a) and (b) exceeds quite a bit the uncertainty value of experimentally determined α given by the CODATA 98. Consequently, the condition for phase repetitions of the two proper frequencies is not fulfilled for three orbital cycles with total trace length of $3 \times 2\pi a_0$. Therefore, we may search for the next smallest number of orbital cycles in which the phase repetition conditions are satisfied. It stands to reason that the approximate value of the orbital cycles could be about 137 ($1/\alpha$). Then if not considering relativistic correction, the corresponding number of electron turns is $(1 - \alpha^2)/\alpha^3$. When applying a relativistic correction (multiplying by the estimated above gamma factor for the kinetic energy of 13.6 eV) the number of the electron turns becomes $1/\alpha^3$. The phase repetition conditions will be satisfied if this number is integer. Substituting α by its value from CODATA 98 we get: $1/\alpha^3 = 2573380.57$

It is interesting to mention, that the closest integer value of 2573380 is obtained by Michael Wales, using a completely different method for analysis of the electron behavior (See Michael Wales book "Quantum theory; Alternative perspectives", www.fervor.demon.co.uk).

We may use one additional consideration, for validation of the above obtained number. The number of turns multiplied by the time for one turn (the Compton time) will give the total time on the orbit (or the lifetime of the excited state, according to the Quantum Mechanics terminology). If accepting that the total number of turns are 2573380 then we obtain a lifetime of 2.0827×10^{-14}

(s), that appears to be at least two order smaller than the estimated lifetime for some excited states of the atomic hydrogen.

Following the above analysis we may check for phase repetition at $1/\alpha^4$ turns. The participation of α at power of four is in agreement also with the following consideration: In the analysis of the vibrational mode of the molecular hydrogen, an excellent match between the developed model and observed spectra (section 9.7.5 in Chapter 9 of BSM) is obtained if the fine structure constant participates at a power of four. In such case we may accept that the phase repetition conditions is satisfied for a number of turns given by the closest integer in Eq. (3.43.i).

$$1/\alpha^4 = \text{integer} \quad (3.43.h)$$

Using the CODATA value of α we obtain $1/\alpha^4 = 352645779.39$. Rounding to the closest integer we obtain an expression for the theoretical value of α (if its experimental estimation is accurate enough).

$$\alpha = (352645779)^{-1/4} = 7.2973525 \times 10^{-3} \quad (3.43.i)$$

The small difference of the theoretically obtained value of α from the experimental one could be caused by an experimental error. One of the methods for accurate experimental estimation of α is based on the measurement of the Josephson constant, K_J . Its connection to α is given by the expression

$$K_J = \frac{2}{c} \left(\frac{2\alpha}{\mu_0 m_e \lambda_c} \right)^{1/2}$$

where: μ_0 - is the permeability of vacuum, m_e - is the electron mass, c - is the light velocity, λ_c - is the Compton wavelength.

The accuracy of α according to this method depends mostly on the accuracy of the Josephson constant measurement, because all other parameters are accurately known. The recommended value for this constant according to CODATA 98 is $K_J = 483597.898(19) \times 10^9$ (Hz/V). If replacing α in the above expression of K_J with the value obtained

by Eq. (3.43.i) we will get the value of K_j that is in the uncertainty range given by the CODATA 98.

The conclusion that the orbital time duration may depends only on α is reinforced also by the consideration that the Compton wavelength, λ_c , was initially involved in the analysis (Eq. (3.43.d), (3.43.e), (3.43.f)), but it disappeared in the derived Eq. (3.43.i). Consequently, the phase repetition condition is satisfied not only for the two proper frequencies of the electron, but also for the SPM frequency of the CL nodes included in the quantum orbit (λ_c is the propagated with a speed of light phase of the SPM vector for one SPM cycle of the CL node (SPM frequency = Compton frequency)).

In §3.5 it was described, that the central core is moving in the CL zone of magnetic quasispheres (MQ's). When the quantum loop condition is satisfied, the phase of core motion appears as repeatable in respect to the stationary CL nodes. The arrangement of MQs along the orbit trace will have a helical shape. This is illustrated in Fig. 3.20.

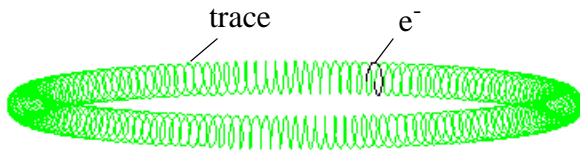


Fig. 3.20

Electron motion in quantum loop. MQ trace is shown by green line with a shape of close loop helix. The momentary position of the electron structure is shown as a black single turn

It looks like the motion of the electron system is like a screwing in a helical curve. The MQs along this helical curve possess a strictly determined spatial order.

There are following important features of the electron motion in such conditions:

(1) The phase difference between the stationary MQs along helical curve and the oscillating central core is zero for any point in the curve.

((2) In the absence of external electrical and magnetic field, there is not a phase dephasing in the closed loop of the aligned MQs, i. e.

there is not disturbing interactions caused by the CL space environments.

(2) In presence of external electrical or magnetic field up to some limit, the electron orbit could exhibit self adjusted properties.

The second feature, is valid only in the absence of external electrical field. The “near field” of the electrical field of the proton, for example, exhibits spatial configuration. In such conditions, the above feature becomes valid only for the boundary orbit. For other orbits, the total phase sum is preserved, but continuous phase difference appears, as a running phase in the closed helical curve. This causes a phase shift in the helical loop of MQs and **creation of magnetic line**. This effect will be additionally discussed in Chapter 7.

One question here may arise: The MQs oscillate with SPM frequency equal to the Compton one, while the positron - core frequency is three time higher? How the phase can be kept close to zero in this case?. The explanation is in the SPM vector quasisphere. From the spatial point of view, the bumps are much narrower, than the sinusoids. From the temporal point of view, however, they are much wider, because, the SPM vector spends much more time in the bumps. Fig. 3.21 illustrates the interaction process between the oscillating central core and one of the MQ bumps, unfolded in time. The time diagram should be considered in frame travelling with the electron.

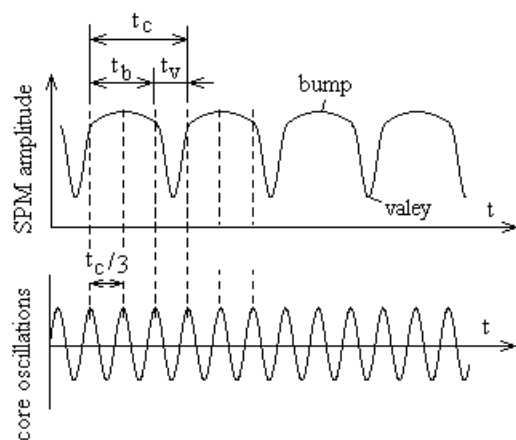


Fig. 3.21

Interaction between central core and SPM vector of stationary MQ nodes

The interaction between the two oscillations with different but constant ratio of their frequencies

is possible due to the ratio $t_b/t_v > 1$, where t_b is a bump time and t_v is valley time of the SPM vector.

The provided concept of the fine structure constant embedded in the quantum loop, which defines the quantum orbit matches to the analysis of Balmer series in Hydrogen, provided in Chapter 7, where α is involved in the **orbital time of the electron** (time duration of the electron circling in one quantum orbit).

3.12.2.A. Quantum orbits and time duration for a stable orbit

It is apparent from the provided analysis that a stable quantum loop is defined by the repeatable motion of oscillating electron. The shape of such loop, however, is determined by external conditions. Such conditions may exist in the following two cases:

- a quantum loop obtained between particle with equal but opposite charges and same mass, as in the case of positronium (see Chapter 3 of BSM)
- a quantum loop obtained between opposite charged particles but with different masses (a hydrogen atom as a most simple case and other atoms and ions as more complex cases).

In both options the quantum loops are repeatable and we may consider that any quantum orbit is formed of whole number of quantum loops.

A single quantum orbit could contain one or few serially connected quantum loops (in both cases the condition for phases repetition is preserved). It is obvious that the shape of the quantum orbit is defined by the proximity field configuration of the proton (or protons). The vacuum space concept of BSM allows unveiling not only the electron structure but also the physical shape of the proton with its proximity electrical field (chapters 6 and 7 of BSM). The shape of any possible quantum orbit is strictly defined by the finite geometrical parameters of the proton.

Let considering now the induced magnetic field of the electron motion in a quantum orbit by using the electron magnetic radius. The magnetic radius of the electron moving with different subharmonic numbers n is analyzed in section 3.1, Chapter 3 of BSM. Its value for $n = 1$ (a kinetic energy of 13.6 eV) matches the estimated magnetic

radius corresponding to the magnetic moment of the electron. For larger numbers (decreased electron energy), however, the magnetic radius shows an increase. The physical explanation by BSM is that at decreased rate of the electron rotation its IG field of the twisted internal RL structure is able to modulate the surrounding CL space up to a larger radius until the rotating modulation of the circumference reaches the speed of light. Keeping in mind that the circumference of the electron is equal to the Compton wavelength (with a first order approximation) the circumference length of the boundary (defined by the rotation rate) should be a whole number of Compton wavelengths. Then the integer number of the Compton wavelengths corresponds to integer subharmonic number. In such case, the orbiting electron with optimal or sub-optimal velocity could not cause external magnetic field beyond some distance from the nucleus. This provides boundary conditions for the atoms, if accepting that in any quantum orbit the electron is moving with optimal or sub-optimal confined velocity (integer sub-harmonic number). Here we must open a bracket that the higher energy levels in heavier elements come not from a larger electron velocity but from the shrunk CL space affected by the accumulated protons and neutrons. Such CL space domain is pumped to larger energy levels in comparison to the CL space surrounding the hydrogen atom.

The existence of the IG law changes significantly the picture of the orbiting electron in a proximity field of the proton. In Chapter 7 of BSM an analysis of Balmer model of Hydrogen atom is developed based on the BSM concept of the electron and proton and the IG law influence on the orbital electron motion in the proximity to the proton. It appears that the limiting orbit has a length of while all other quantum orbits are inferior. This conclusion is valid not only for the Balmer series in Hydrogen but also for all possible quantum orbits in different atoms, if they are able to provide line spectra. Therefore, the obtained physical model of Hydrogen puts a light for solving the boundary conditions problem of the electron orbits in the atoms.

Time duration for a stable orbit (lifetime of excited state).

The following analysis could be valid only for the hydrogen, where the influence of the proton mass on the surrounding CL space appears to be negligible.

Keeping in mind the screw-like confined motion, the axial and tangential velocities will be inverse proportional to the subharmonic number. Then the condition for phase repetitions for a motion with a subharmonic number n will be satisfied for n times smaller number of electron turns, or the quantum orbit will be n times smaller. It is reasonable to consider that the first and second proper frequencies of the electron are stable and not dependent on the subharmonic numbers. Then for estimation of the time duration of the orbit (the lifetime of excited state) it is more convenient to use the number of the cycles of the first proper frequency of the electron. It is equal to the number of electron turns for $n = 1$. In such way we arrive to the conclusion:

(a) If conditions for stable quantum orbit are defined only by the phase repetition conditions and the whole number of Compton wavelengths, the time duration (lifetime) of the orbiting electron does not depend on the subharmonic number of its motion.

(b) If (a) is valid, the lifetime of the excited state will be equal to the product of the total number of the first proper frequency electron cycles (according to Eq. (3.43.h)) and the Compton time (the time for one electron cycle with the first proper frequency).

According to condition (b) the theoretical lifetime for an excited state of the hydrogen is

$$\tau = t_c / \alpha^4 = \lambda_c / (c\alpha^4) = 2.85407 \times 10^{-12} \text{ (s)} \quad (3.43.k)$$

where: $t_c = 1/v_c$ - is the Compton time.

Note: The obtained Eq. (3.43.k) does not take into account the possible modification of the surrounding space in a close proximity to the proton. Such modification (a slight shrinkage, or a space curvature) may cause aliasing for the phase repetition conditions due to affected SPM frequency and Compton wavelength, while the first and second proper frequencies of the electron are obviously stable. For heavier atoms such modification may appear much stronger. For elements with more than one electron, the mutual orbital interactions also may lead to increase of the real lifetime.

3.12.3 Quantum loops and orbits, for electron with any suboptimal quantum velocity

The analysis so far was done for an optimal confined motion - first harmonic quantum motion. Let to see, how the quantum loop condition is satisfied for motions with subharmonics.

If the electron is moving with a second subharmonic, its velocity is two times slower. The positron - core system will make the same number of oscillations for twice shorter path. Consequently the same conditions for a quantum orbit are satisfied for twice shorter orbit. For quantum motion with n subharmonic the quantum loop will be n time shorter. This conclusion is evident also by the Eq. (3.43.d). Then the length of the quantum orbit, L_{qo} , may be expressed by the equation:

$$L_{qo}(n) = \frac{2\pi a_o}{n} = \frac{\lambda_c}{\alpha n} \quad (3.43.j)$$

where: n - is the subharmonic number

In a similar way as we used the term subharmonics for the quantum motion of the electron, we may use it again for the quantum loop. Then the first harmonic quantum loop corresponds to electron motion with energy 13.6 eV, the second harmonic quantum loop - to 3.4 eV and so on.

The orbit shape in the quantum loop is not important. The quantum loops are very important features of the electron motion around the proton in the atoms. When discussing the Hydrogen orbits in Chapter., we will see, that they are folded 3D curves.

The quantum orbits play important role, also, between the atomic connections in the molecules. In this aspect additional combinations of the quantum loops are possible: **Two or more quantum loops can be connected in serial, giving a longer quantum loop.** Such loops are possible in the atomic nuclei and between atoms. Experimental evidence for such loop exists, by the observed "series" in the photoelectron spectra. This will be discussed in Chapter...

Summary:

- **The quantum orbits are closed loop electron trajectories, containing whole number of central core oscillation periods**
- **The central core trace in the quantum loop is a helix of aligned MQs.**

- **In absence of external electrical field, there is not distributed phase shift between aligned MQs and the CL space MQs.**
- **When the quantum loop is spatially matched to external electrical field, a dephasing appears between the loop aligned MQs and external CL space MQs. This means that the MQs in the helix are connected in magnetic line.**
- **The characteristic parameter of the quantum orbit is the orbit length, so its shape does not need to be circular.**
- **The quantum orbits are possible for the first harmonic and subharmonic quantum velocities. Consequently the attribute n-subharmonic quantum orbit is completely adequate.**
- **The length of the n-subharmonic orbit is n times shorter, than the length of the first harmonic (optimal confined velocity).**
- **Subharmonic quantum loops are able to be connected in series, forming a common quantum orbit.**

3.13 Estimation of basic CL parameters by the parameters of the electron system. Derivation of the mass equation.

3.13.1 Physical interpretation of inertial mass ratio

In Chapter 6 the similarity between the electron and muon (and positron and muon) is discussed. The muon is a second order structure whose central radius is the same as the electron radius R_e . The evidence of this comes from the fact that the muon can oscillate longitudinally and when it crashes, only a single coil could be left from one of its edges. All other portion of the muon helical structure together with its internal lattice is disintegrated finally as neutrino. When providing a physical interpretation of the mass and magnetic moment magnetic moment we come to the conclusion that the muon has 206.7 more windings than the electron system. Then their volume ratio of their FOHS is also equal to this value. It follows, that the inertial mass of the muon is equal to the inertial mass of the electron multiplied by their volume ratio that is 206.7. This can be expressed by the equation:

$$\frac{\mu_e}{\mu_\mu} = \frac{m_\mu}{m_e} = 206.76 = \frac{206.76 \text{ windings}}{1 \text{ winding}} \quad (3.44)$$

From Eq. (3.44) follows, that there is direct proportionality between the amount of the FOHS in the helical structures and their apparent mass.

The ratio equivalence between the mass and magnetic moment is valid only for the similar helical structures. The same ratio, for example is not valid between the electron and proton or neutron. The latter two particles are formed of higher orders helical structures. They also have confined motion, but, but due to a equivalent high order helicity. However, all helical structures exhibiting confined motion, contain FOHS.

From the considerations discussed above, the following conclusions can be made:

The inertial mass of any helical structure, exhibiting confined motion, could be expressed by the electron mass multiplied by the ratio between the volumes of their first order helical structures.

3.13.2 Relation between CL node displacement from FOHS and the Broglie wavelength

Accepting the apparent mass of the electron system as unity, we will derive equation that relates its mass to the cosmic lattice parameters.

The mass to magnetic moment ratio is valid for similar structures like electron (positron) and muon. Similar expression between the electron and proton is not valid, because their shapes are different. However there is some similarity in the behaviour of their structure. This is the confined motion and we will use this feature in the following analysis.

It is well known fact, that the elementary particles exhibit a wavelike motion with wavelength determined by the Broglie equation:

$$\lambda = \frac{h}{mv} \quad (3.44.a)$$

where: λ - is the wavelength of the wave like motion

m - is the particle mass

v - is the particle velocity

Now we will give the physical interpretation of this equation from the point of view of prisms

theory. It was pointed out that the confine motion of the proton and neutron is due to their equivalent helical step. The confine motion means that the particle rotates. Consequently there is some periodicity of the particle interaction with the lattice. This periodicity will depend of the particle mass, the motion velocity and ability of the particle to twist the lattice. All this parameters are contained in the Broglie equation. The important feature of this equation is that the mass is involved, and this will give us a key for derivation of the inertial mass equation. Let to apply this equation for the electron, in case when $v = c$, and make some manipulations, as shown in eq. (3.44.b).

$$\lambda = \frac{h}{m_e c} = \frac{h \cdot c}{m_e c c} = \frac{hc}{h v_c} = \frac{c}{v_c} \quad (3.44.b)$$

Now manipulating the dimensions of (3.44.a) and (3.44.b) we get:

$$wavelength = \frac{N m sec}{kg m sec^{-1}} = \frac{N m}{kg m sec^{-2}} = \frac{torque}{force} \quad (3.45)$$

From Eq. (3.44.a) we see that λ becomes the wavelength of the SPM frequency (Compton frequency in Earth local field) $v_{SPM MQ}$ when $v = c$.

From dimensional interpretation of Eqs. (3.44.a) and (3.44.b), shown as Eq. (3.45), we see that the Broglie wavelength can be expressed as a ratio of torque over force that moves the particle. The torque is a result from the particle helicity.

The waves from particle having confined motion could be regarded as a dynamical lattice disturbance. The wavelength of this disturbance is equal to the torque that the particle exercise on the lattice under the pushing force. The expression for this type of disturbance is valid for real velocity, without taking into account the relativistic mass change.

The inertial mass can be regarded as a static lattice disturbance causing a lattice displacement. Interpolating the Broglie expression to motion with light velocity without taking into account the relativistic mass change, provides the inertial mass.

Having in mind that the optimal confined motion of the electron is completely determined by its geometry and the fundamental frequency, we can make the following general conclusions:

- The electron system could serve as inertial mass unit in the lattice measurement system.

- The mass of the electron system can be expressed by the lattice parameters, system geometry and fundamental frequency.

3.13.3 Static CL pressure and apparent (Newtonian) mass of the helical structures

It has been already mentioned, that the Compton frequency is a value of the SPM frequency at Earth local field. Let to express the electron inertial mass from the Eq. (3.44.a), when $v = c$ and apply some manipulation of the dimensions.

$$m_e = \frac{h}{\lambda c} \quad (3.46)$$

$$\frac{Nmsec \cdot m^2}{mmsec^{-1}m^2} = \frac{N}{m^2} \frac{m^3}{m^2 sec^{-2}} = \frac{(pressure) \times (ref. volume)}{(light velocity)^2} \quad (3.47)$$

From the dimensional equation (3.45) we see, that the inertial mass can be expressed by the parameters shown in the brackets. Then the **equation for the inertial mass** of helical structure exhibiting confined motion, will take a form given by (3.48).

$$m = \frac{P_S}{c^2} V_{H(SI)} \quad (3.48)$$

where: P_S - is the cosmic lattice static pressure on the

external shell of FOHS

$V_{H(SI)}$ - is the FOHS volume referenced to the measuring system (SI in this case)

c - is the light velocity

Based on the Eq. (3.48) we can formulate the inertial mass in the cosmic lattice space:

- The inertial mass of particle in the lattice space is proportional to the static lattice pressure and the volume of FOHS's contained in the particle, and inverse proportional to the square of light velocity.

The inertial mass of helical structure with second order helicity is equal to its gravitational mass. So we may refer it as a **Newtonian mass (or Newton's mass)**. The Newtonian mass is different than the intrinsic mass. **It does not take into account the amount of the intrinsic matter inside of its FOHS.**

The pressure P_S is called static, because the CL nodes are constantly displaced by the volume of the FOHS. This volume is occupied by RL(T) and even folded nodes could not pass through. The

electron system contains only single coils of FOHS (external negative and internal positive). Knowing the total volume occupied by the RL(T) we can estimate the static pressure, P_S , by applying Eq. (3.48)

$$P_S = \frac{m_e c^2}{V_{e(SI)}} \quad \frac{N}{m^2} \quad (3.49)$$

where: $V_{e(SI)}$ is the electron volume, expressed in units of SI

From Einstein mass - energy equation we have:

$$m_e c^2 = h\nu_o = 511 \text{ KeV}/c^2 \quad (3.50)$$

Then the static CL pressure, can be expressed also by Eq. (3.51).

$$P_S = \frac{h\nu_o}{V_{e(SI)}} \quad \left[\frac{N}{m^2} \right] \quad (3.51)$$

Checking the dimensional correctness of Eq. (3.51) we get:

$$\text{pressure} = \frac{N}{m^2} \left(\frac{m\text{sec}}{m\text{sec}} \right) = \frac{Nm\text{sec}}{m^3} \frac{1}{\text{sec}} = \frac{Nm\text{sec}}{m^3} Hz \quad (3.52)$$

The accepted in §3.6 relation $s_e = g_e r_e$ matches well with all the calculations, physical considerations and models developed by BSM. Having in mind the relation between R_c and s_e , given by Eq. (3.9), we may express the static pressure only by the CL parameters. We have two options for this purpose: by the SPM (Compton) frequency or by the resonance frequency:

The **static CL pressure**, when using the SPM (Compton) frequency is:

$$P_S = \frac{h\nu_c^4 g_e^2 (1 - \alpha^2)}{\pi \alpha^2 c^3} = 1.37358 \times 10^{26} \quad \left[\frac{N}{m^2} \right] \quad (3.53)$$

where: α - is the fine structure constant, g_e - is the electron giromagnetic factor

The **static CL pressure**, when using the resonance parameters is:

$$P_S = \frac{h g_e^2 (1 - \alpha^2) \nu_R k_{hb}^3}{\pi \alpha^2 N_{RQ}^4 d_{nb}^3} \quad \left[\frac{N}{m^2} \right] \quad (3.54)$$

where: d_{nb} - is the node distance for not disturbed CL field; ν_R - is the node resonance frequency; N_{RQ} - is the number of resonance cycles for one SPM MQ cycle

k_{hb} - is the quantum wave boundary condition factor, given by Eq. (2.20.a):

$$k_{hb} = \sqrt{1 + 4\pi^2(0.6164^2)} = 4 \quad ,$$

where: 0.6164 - is a factor complying to the Rayleigh criterion

The ratio m_e/V_e in Eq. (3.49) could be regarded as a mass density of the electron. A single coil from muon has the same mass density. The pion and kaon structures could be also referenced to this value. Comparing Eq. (3.49) and (3.53) we see, that the mass density of the electron is:

$$\rho_e = \frac{m_e}{V_e} = \frac{g_e^2 h \nu_c^4 (1 - \alpha^2)}{\pi \alpha^2 c^5} = 1.528315 \times 10^9 \quad \left[\frac{kg}{m^3} \right] \quad (3.55)$$

Then the CL static pressure obtains a simple form:

$$P_S = \rho_e c^2 \quad (3.56)$$

The expression (3.56), is quite convenient especially in the analysis of the inertial features of the particles and macro systems in CL space and their relativistic features. Such analysis is presented in Chapter 10.

Eqs. (3.51), (3.53) and (3.54) are fully consistent and give one and a same value of CL static pressure:

$$P_S = 1.373581 \times 10^{26} \quad [N/m^2]$$

We might be surprised, in a first gland, that P_S has so large value. If estimating also the total force exercised on the electron surface S_e we will find that it is quite large. But this an area where large energy interactions takes place. The interactions involving the CL static pressure however are static and we can not feel them. We can feel them and detect them when change of the FOHS takes place. Two type of changes exists for the electron system: (a) separation of the positive (internal) from the negative negative (external) FOHS's; or (b) destruction of the system. This topic is discussed in Chapter 6.

Substituting the value of P_S in Eq. (3.48) and knowing the volume of the FOHS involved in the particle, we can calculate its apparent mass in CL space, referred as Newtonian mass according to BSM.

Mass definition:

- **The newtonian mass of any helical system in CL space, exhibiting confined motion, could**

be determined by the fundamental parameters h , v_o , c , and the total volume of its first order helical structures.

By substituting P_S from one of Eq. (3.51), (3.53) or (3.54) into Eq. (3.48) we obtain the mass equation, estimated by the CL space parameters and the FOHS volume.

$$m = \frac{g_e^2 h v_c^4 (1 - \alpha^2)}{\pi \alpha^2 c^5} V \quad [\text{kg}] \quad (3.57)$$

where: V_{HS} is the volume of the FOHS

Note: The mass Eq. (3.57) in this form is valid only for negative FOHS's. For positive FOHS's the volume, the proper frequency and the tangential to axial velocity ratio are different. This requires use of correction factor (see §3.14).

- **When the mass equation is applied for the positive FOHS the right side of the mass equation should get a multiplication factor of 2.25.**

It is evident from Eq. (3.48) that the mass of any helical structure, is determined by the volume of all of its FOHS's. The electron system contains only one coil of combined (positive inside a negative) FOHS. Consequently, it is a suitable mass unit for estimation the mass of more complex structures. Sometimes another task is more useful - determination of the dimensions, when the mass ratio is known. In this case another form of the mass equation is more suitable. Substituting (3.51) in (3.48) and introducing the volume normalisation factor K_V **the newtonian mass equation** takes a form:

$$m = \frac{h v_c}{c^2} K_V \quad [\text{kg}] \quad (3.58)$$

where:

$$K_V = \frac{V_{H(SI)}}{V_{e(SI)}} = \frac{V_H}{V_e} \quad (3.59)$$

K_V is a ratio between the total volume of all FOHS's of the particle with mass m and the electron volume.

Note: The mass equation (3.58) is valid for negative FOHS's.

For newtonian mass of positive FOHS's, we must use the positron estimate of the Plank's constant and the positron's proper frequency. In the

next paragraph (§3.14) it is shown, that the product of both parameters is

$$h' v_{pc} = \left(\frac{9}{8}h\right)(2v_c) = 2.25h v_c \quad (3.59.a)$$

Consequently, when applying the mass equation for positive FOHS's the factor 2.25 should be used in the nominator.

The Eq. (3.58) provides results, consistent with the practically estimated masses of the following particles: proton, neutron, pion, muon. They all have second order helicity. The experimentally estimated masses of the kaons are not consistent with the calculated masses by the mass equation. The kaon is strait FOHS, but this is not the main reason. The reason is the following:

The mass of the kaon is not correctly estimated in the experiments in the particle accelerators, because it possesses active jet during its lifetime. This jet is from destructing internal RL(R) or RL(T) structures providing reactive forces for its motion. If these forces are not taken into account the kaon mass is overestimated. The calculations in Chapter 6 shows that the kaon mass is overestimated 11 times. The pulsar theory presented in Chapter 12 also confirms the evidence of the jet of single kaon in CL space.

The mass equation is valid for any single particle up to the size of the proton (neutron). However it is not exactly valid for the atomic nuclei, larger, than Hydrogen. When the number of protons and neutrons, forming the atomic nuclei, increases, a mass deficiency effect appears due to the shrinkage of the CL space around the nuclei from the IG(CP) forces (effect of general relativity). In such case the atomic mass appears slightly lower than the sum of the neutrons and protons masses. The mass difference between the apparent mass and the summation of the protons and neutrons is known as a bonding energy.

Summary notes:

- The static pressure of cosmic lattice is the pressure exercised on the surface of the first order helical structure.
- The electron is a convenient helical structure for estimation of the CL static pressure.
- The apparent mass of a first order helical structure is equal to the product of the static pressure

and the structure volume, divided by the square of the light velocity

- The mass of any single helical structure is completely determined by the total volume of its FOHS's.
- The inertial mass of a particle containing FOHS is completely defined by the CL space parameters, without presence of external gravitational field.

3.13.4. Physical nature of inertia and inertial mass

The inertia can be regarded as an effect preventing the helical structures to get infinite acceleration. This is a result of increased interaction between the field of the internal RL(T) and the oscillating nodes of the CL space.

Any particle is consisted of helical structures. Any type of helical structure is build of FOHS that may be curled into second and third order helical structure. Only FOHS contains internal RL(R) or RL(T). They both are much denser than the CL structure. So the node of CL space could not penetrate inside the FOHS. The excess CL nodes are folded and placed among the CL nodes. They form the dynamical CL pressure. The motion of any FOHS through the CL space, however, causes continuous folding and unfolding of CL nodes. In this process the both type of pressures are constant. From the point of view of the moving FOHS the static pressure is a scalar, while the dynamical pressure is a vector. The parameter of the dynamical pressure, that determines it as a vector is the direction of motion. It is involved in the definition of the inertia for any particle comprised of helical structures. In such aspect the inertial mass could be expressed by the equivalent interaction energy in CL space: $E = mc^2$. The gravitational mass is measurable only if gravitational interaction exists. It also have equivalent energy in CL space. A normal CL space assures equivalence between the inertial and gravitational mass for all type of helical structures.

The inertial properties of particles and macrobodies are discussed in Chapter 10.

3.14. Free positron. Newtonian mass and Planck's constant estimated by its motion in CL space.

It is experimentally known fact, that the masses of the electron and positron are exactly equal. Then the Planck's constant should have different estimate by the Positron parameters. In §3.14 it was concluded, that, the proper frequency of the free positron is twice the proper frequency of the electron system (Compton frequency), or $v_{pc} = 2v_c$. Having in mind the volume ratio of the electron - positron $K_V = r_{pc}^2/r_e^2 = 4/9$ we may express the positron mass.

$$m_{pos} = \frac{h'v_{pc}4}{c^2 \cdot 9}$$

Equalising the positron and electron masses we get:

$$h' = (9/8)h \quad (3.50)$$

where; h' - is the Planck's constant estimated by the positron parameters; v_{pc} - is the proper frequency of the free positron system, equal to twice the Compton frequency

$$h'v_{pc} = 2.25hv_c \quad (3.50.a)$$

Eq. (3.50.a) shows, that when the mass equation is applied for the positive FOHS, the product $h'v_{pc}$ is valid, or the equation should get a multiplication factor of 2.25.

3.15 Dynamic pressure of CL space

In Chapter 2 it was discussed, that the background uniformity of the CL space is maintained by zero order waves. This wave are related with the spontaneous creation of magnetic protodomains, whose concentration is a constant parameter. In all these effects the CL relaxation constant is involved. Its accepted theoretical value was discussed in Chapter 2, §2.13B. The reciprocal value of the relaxation constant has a dimension of frequency. It could be called relaxation quasifrequency, because it is not defined by exact periodical motion. It is given by the equation:

$$v_{CL} = \frac{1}{t_{CL}} = \frac{v_c}{(c)} = 4.12148 \times 10^{11} \quad [\text{Hz}] \quad (3.60)$$

where: (c) - is a light velocity as a dimensionless factor

Defined in this way, we may use the relaxation quasifrequency only in the same measuring system - the system SI.

In a similar way as the static pressure, given by Eq. (3.51), we define a dynamic pressure, that, however, is referenced to the relaxation quasifrequency of CL space, given by Eq. (3.60). The dynamic pressure is caused by zero point waves, with wavetrain length of λ_c . Consequently they may envelope around the electron or positron, but could not penetrate inside the FOHS volume. So they may exercise forces on the envelope of the helical structures. For this reason the surface of the external electron shell will be used for a reference. The dimensions of this pressure should be: $\left[\frac{N}{m^2Hz}\right]$. Then the equation of the dynamical pressure is:

$$P_D = \frac{h}{c} \frac{v_c}{S_{e(SI)}} = 2.025786 \times 10^3 \left[\frac{N}{m^2Hz}\right] \quad (3.61)$$

where: $S_{e(SI)}$ - is the surface of the electron's external shell envelope

The correct dimensions of Eq. (3.61) appear when the light velocity participates with its dimensions. For this reason the brackets used in Eq. (3.60) are not used in Eq. (3.61).

The dimension of the Eq. (3.61) is a "pressure unit per frequency". For this reason it is called dynamical pressure. When applied to the envelope of a helical structure it exercises an alternative force with a frequency given by Eq. (3.60).

The Dynamical pressure is a pure CL space parameter as the static pressure. for this reason it could be expressed only by physical constants:

$$P_D = \frac{g_e h v_c^3 \sqrt{1 - \alpha^2}}{2\pi\alpha c^3} \quad (3.62)$$

where: g_e - is the electron giromagnetic factor
Eq. (3.62) gives exactly the same value as Eq. (3.61).

Note: The dynamic pressure, is equally applicable for a negative and positive external shells, and is not influenced by the type of the internal structures. The static pressure, however, has different value for negative and positive FOHS's, and this should be taken into account, when applying the mass equation. The latter conclusion is confirmed by the calculations for the dimensions of the proton and its substructures.

The dynamical pressure provides a way for indirect estimation of the ZPE by the measurement of the behaviour of an atom, that is in equilibrium conditions. This approach is used in Chapter 5 for calculation of the background temperature of deep CL. It corresponds to the experimentally determined parameter known as Cosmic Microwave Background.

3.16 Scattering experiments for electron and positron from the point of view of the BSM theory.

The reader perhaps is aware of the large discrepancy between the Compton radius of the electron and the radius determined by the scattering experiments (scattering radius). While the Compton radius is 3.86E-13, the scattering experiments give the value about 1E-16. This huge discrepancy is solved by the BSM theory.

The "electron - electron" scattering model is developed by C. Moller (1932) and the process is known as a Moller scattering. The electron - positron scattering equation is derived by H. J. Babha and the process is known as a Babha scattering. Later modifications, based on the Dirac theory are applied involving correction for the spin. Some improvements are also contributed by Scott, 1951; Barber, 1953; Ashkin, 1954 and others. The Moller and Babha equations has been corrected, but the basic assumption is not changed. The basic assumption for both type of scattering is that the electron and positron are regarded as a point like particles possessing a charge. The scattering models takes into account the kinetic energy of the both particles and allows to determine the angular distribution and the differential scattering cross section. From this data one can determine the size of the electron with a priori accepted shape and features.

Let to the Babha scattering model for example. The following parameters are taken into account: electron (positron) mass, electrical charge, velocity, spherical radius, two spin parameters (+h and -h).

Fig. 3.22 shows the angular distribution of scattering events for Babha scattering at 29 GeV (D. Bender et al., (1984). In the same figure the

theoretical curve with Monte Carlo simulation is shown.

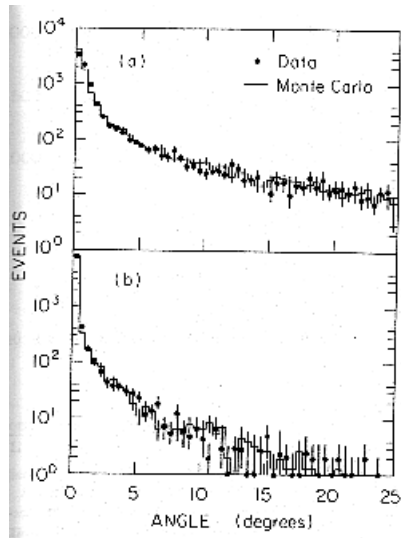


Fig. 3.22

Angular distribution of scattering events for Babha scattering at 29 GeV (D. Bender et al, 1984)

The ordinate is in logarithmic scale because the peak is very sharp. When assuming a spherical shape, the data of the scattering experiment lead to a result, that the radius of the sphere is very small - in order of $1E-16 m$. The existing so far theories are not able to explain the huge discrepancy between the Compton radius $R_c = 3.86159 \times 10^{-13} m$, and the scattering one.

From the point of view of the BSM, the discrepancy between the Compton and scattering radius of the electron, come mainly from the assumption, that the electron does not possess a structure. In the Moller and Babha scattering models, the following factors are not taken into account:

a. The form factor: a sphere is assumed, instead of single coil of first order helical structure.

b. The confined motion in CL space

c. The oscillation properties of the electron subsystems

d. The possibility for different rotational phase at the moment of meeting in the high energy collision

e. The intrinsic gravitation between the helical structure

f. The distributed charge appearance in close encounter

It is evident, that the result could be quite different, if obtaining a scattering model with all this factors. The model in this case, however, could be quite complicated.

Fig. 2.23 illustrates the scattering process according to the Moller and Babha assumptions - case **a.**, and BSM - case **b.**.

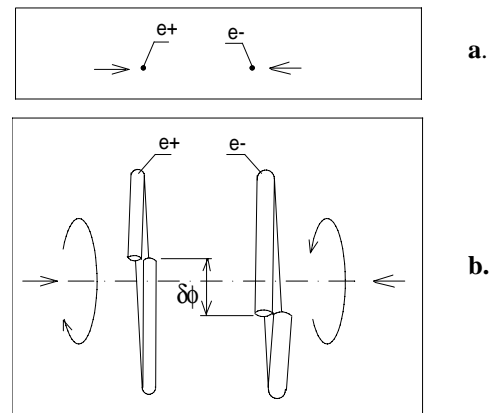


Fig. 3.23

Electron positron scattering according to: a. Babha model; b. Twisted prisms theory

Fig. 3.23.b illustrates the orientation, spin direction and the phase difference $\delta\phi$ in the moment of meeting.

In the Babha model the spin moment has only two values ($+h/2$ and $-h/2$). The both values may express correctly the quantum energy, but only for motions with suboptimal velocities. In the Moller and Babha scattering, the velocities are much higher, so the quantum motion effect, according to BSM is significantly reduced. Then it is not correct to use the same spin momentum as in the low energy motion.

3.17 Positronium

The positronium is a state of temporally stable combination, between the helical structures of a whole or refurbished electron system, or virtual quasiparticle, able to pump the CL space. In the end of oscillating process a photon is emitted. The duration of the oscillation is known as a lifetime. **According to BSM, only the far field electrical charges disappear, but the mass of the system does not annihilate.**

A pretty large number of combinations are possible, but we can list here a few of them, for which experimental evidence exists:

- $Ps1^1S_0$ state
- $Ps1^3S_1$ triplet
- $Ps\ 1^3S_1 - 2^3S_1$ singlet
- Ps^- -"positronium negative ion"

3.17.1 $Ps1^1S_0$ state

This state involves oscillations between a normal electron and a free positron. The free positron is directed toward the internal positron, and both positron start to oscillate as a common system in the electron shell. The oscillation process provide a CL pumping and terminates with emission of two polarized gamma quant of 511 in opposite direction. The obtained common helical structure is comprised of the electron shell and two halves of the positron shells. The opposite E-fields are locked in the proximity (by the IG field) and the final (quiet) system appears as a neutral. Such system is very difficult for detection. The process is known as "annihilation" but we see, that the matter is not annihilated.

3.17.2 $Ps1^3S_1$ triplet

This state is usually activated when a positive Beta particle from radioactive decay starts to oscillate with a normal electron system. The Beta particle is a quasiparticle wave, possessing a positive charge of running EQs moving as a quantum wave. This type of wave does not have strong boundary conditions and behaves as an electrical charge. The radial dimension of this wave is a function of its energy. Smaller energy means larger radius. When the quasiparticle wave meets the electron system their electrical fields interact and cause multiple repeatable oscillations of the electron - positron system. In a such process a lattice space pumping effect occurs. During the pumping process the energy of the quasiparticle, that have been distributed only among the positive EQs, redistributes between the positive and negative EQ'. In result of this the positive charge is gradually consumed, and its energy is converted to a pumped CL space ener-

gy. The latter finally is released as 3 gamma quants, if the Beta particle energy is less than 511 keV. The spectrum of 3 gamma emission is a continuous. Here one question arises: Why 3 gamma quants are emitted?

The explanation is the following:

The most energetic quantum wave is the first harmonic wave with energy of 511 keV. According to the boundary conditions, only subharmonics wave are possible. This condition put a limit on the spectrum continuity in the vicinity of the first harmonic. The quasiparticle wave, however, may poses any value of energy, that do not coincides with the subharmonics quantum conditions. **Such energy could not be presented as sum of two subharmonics quantum wave, but with sum of three subharmonics.**

The described above process is valid for a vacuum or air conditions. When the electron is in solids, the process is modified. The process known as a positron thermalisation belongs to this category. It is discussed in §3.17.5

3.17.3 $Ps\ 1^3S_1 - 2^3S_1$ state

This is a positronium, that terminates with emission of a single photon at 243 nm. One of the experiments in which the above state is activated is provided by Mills, Berko and Canter, (1975).

The transition $1^3S_1 - 2^3S_1$ is obtained by the following way. By moderation of Beta particles from radioactive decay of ^{58}Co , using MgO covered gold foil converter, slow positrons are obtained. These positrons strike MgO covered gold foil converter and then magnetically guided by 150 long curved solenoid strike a copper plate. The copper plate is faced to microwave cavity operating around 8860 MHz. When the microwave (RF) is off, a Ps with a lifetime of 1.1 msec decays in 3 gamma photons. When it is on, emission at 243 nm is detected, in first, and after delay of 1.13 msec a 3 gamma photons are detected.

The explanation of the emission from the point of view of BSM is a following:

The particles obtained by the moderation process are hardware positrons.

Case A. The RF is off.

The slow positrons striking the copper plate are combined to oscillating pair of normal electron - free positron. The oscillation process invokes a CL space pumping and the external E-fields of the

normal electron and the positron become gradually consumed. Approaching a neutral field and possessing kinetic energy they escape easily from the copper plate and enter in the cavity. Here they continue to oscillate with partially lost energy. Their residual energy is lower than 511 keV, because part of it has been exhausted for escaping from the copper plate. In result of this the oscillation process terminates with emission of 3 gamma particles. From the mass point of view, the final system is consisted of two positrons inside of the electron shell with total mass of 1.2 MeV. The positive E - filed of the positron is locked in proximity with the electron field and the particle appears as a neutral. Such particle is very difficult for detection.

Case A. The RF is on.

After the escaping of the the electron - positron system from the copper plate, the process in this case is different. The frequency of the RF filed is suitable for creation of curved loops for both the electron and the positron. They are suitably folded to match the interaction between the moving charge and the magnetic field. In result of this, the two carriers, having still enough energy, do not move directly one to another. In this type of oscillations, supported by the combination of magnetic and RF field, quantum conditions are created, in which the carriers adjust their velocities to 13.6 eV and 3.4 eV. The quantum interaction with the CL spaces allows them to stay longer in this condition. In the same time, the started pumping process continuously degrade the quantum motion in the loops. In some point, they lose the motion in the orbits. Then the CL pumped energy escapes as a photon. The both carriers, now become involved in direct interaction. After 1.1 usec pumping time, the oscillations are gradually suppressed and the accumulated pumped energy is emitted as 3 gamma photons. It is evident that the free positron does not have enough energy to expel the internal positron from the electron system. So the final system is again neutral comprised of one electron shell and two positrons inside.

The RF frequency 8625 MHz appears as an optimal oscillation frequency of the loop. The loop, **however may contain a large number of serially connected first harmonics quantum loops**. This is easily verified by the corresponding period and the known velocity (corresponding to 13.6 eV and

3.4 eV). When approaching this frequency the emission efficiency for 243 nm photons is improved. This curve, reference by the authors as a line is shown in Fig. 3.24.

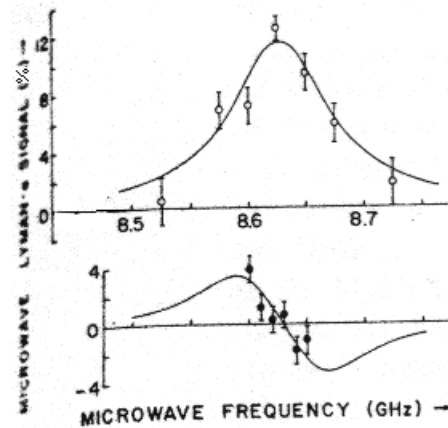


Fig. 3.24

The observed Lyman α signal S (open circles) and logarithmic first-difference signal S^ (solid circles) as a function of microwave frequency (Courtesy of A.P. Mills, Jr. et al.)*

The subharmonic number of the carriers motion in the loops can be easily determined from the photon energy. The only possible combination is: $(13.6 - 3.4)/2 = 5.1$ eV. This means that:

- The quantum motion of the electron corresponds to its first SPM harmonic - optimal confined motion.

- The quantum motion of the free positron satisfies simultaneously two quantum conditions: a second subharmonic of SPM frequency, and a fourth subharmonic of its proper frequency. **This is one additional confirmation, that the proper frequency of the free positron is twice the Compton frequency.** If it was $3v_c$ as the internal positron, such combination could not be possible.

- The lattice pumping effect is result of the energy difference between the two quantum loops, divided in two. The factor of two means 50% pumping efficiency, according to the pumping efficiency Eq. (3.21.c): $\eta = m_e/(m_e + m_e)$.

The axial velocity of the electron is twice the axial velocity of the positron. This condition perhaps makes the lattice pumping effect possible. While the electron motion with optimal velocity is most stable, the positron motion is additionally sta-

bilised by the mentioned above two quantum conditions.

In the same experiment the dependence of the “line” from the RF power is investigated for different power levels. The increase of RF power causes the fitted “line” to move up, giving an impression of broadening, that the authors are not able to explain. According to BSM interpretation this effect is completely logical. Its possible explanation is illustrated by Fig. 3.25 where simple illustrations of the single quantum loops are shown without pretending of their exact shape. In the provided experiment with RF frequency of 8625 MHz, the real orbits lengths should be equal to multiple number of first harmonics quantum loops.

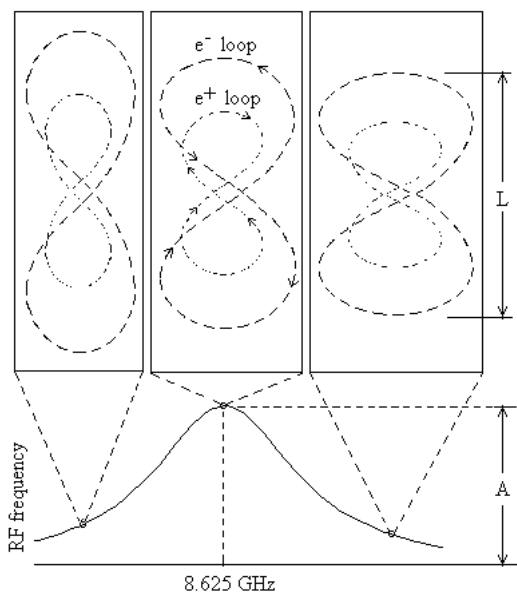


Fig. 3.25

Possible loops of electron and positron motion in $1^3S_1 - 2^3S_1$ state

The RF field in TM010 microwave cavity is parallel to the incident slow positron velocity. Then the formed positroniums also could be preferentially aligned to this field. The RF frequency then will determine the oscillation period of the loop. The carrier velocity in the loop, is fixed by the quantum motion conditions. Then the RF frequency can tune the length of the loop. There is a constant magnetic field of 50 G, however, that fixes the curvature of the trace by the cyclotron radius. This means, that the loop is properly aligned as shown in

the Fig. Then the tuning of RF frequency could make the curve length L shorter or larger, but one optimal value of L should exist. This is the frequency of 8.625 GHz. At this frequency the amplitude of the A parameter of the lorentzian shape is estimated at 11.4%. At different RF power levels of 0.13 mW, 0.41 mW, and 2.0 mW., the corresponding A parameter is 5.3%, 12.3%, and 16.3%. The A parameter is increased, because the larger RF power in the cavity is possible to bias the weak magnetic field, increasing in such way the range of L variation.

3.17.4 Ps^- “Positronium negative ion”

We put the name for this state in bracket, because, it is not a negative ion according to BSM.

According to the existed so far concept the Ps^- state is a combination of one positron and two electrons. Allen P. Mills, Jr. (1983) describes experiment for measuring this state. A beam of 4-eV positrons, produced by ^{58}Co β source and W(110) moderator is guided by a magnetic field to a thin (50 Å) carbon film supported on a NI grid. One of 10^4 positrons emerges from the film as a Ps^- “ion”. It is selected by another grid potential with adjustable distance and then is accelerated by high voltage (regulated between 1 to 4 kV.) The Ps^- is travelling toward Ge(Li) detector with velocity close to the speed of light. This the “annihilation” photons from decay of Ps^- are detected as a blue shifted, and are distinguished from those emitted from the carbon film. The counting rate from this photons increases, when the accelerating voltage is increase. Plots for 1 kV and 4 kV are given.

The interpretation of the experimental data according to BSM is the following.

When the slow positrons from the moderator pass through the carbon film, some of them, interact with the electrons. Not all of the free positrons are combined to a free positron - electron pair. Some of the positrons may only activate the oscillation of the internal positron of the electron system, dissipating lot of obtained energy but do not forming oscillating pairs. The activated in such case electron system may obtain a **strong oscillation mode** (between the electron shell and the internal positron). In this case it may simultaneously exhibit a negative charge (from the electron shell)

and oscillating wave function with Compton frequency. In the far external field it still behave as a negative charge particle and is selected as such by the system of grids and the accelerating electrical field. During the acceleration the oscillating electron gets additional energy. So above some threshold of the applied high voltage its total energy may become larger than 511 MeV. Then the obtained strong oscillations are able to pump the CL space with energy enough for final emission of two gamma photons at 511 keV. The Doppler shifted gamma photons indicate that the end of the pumping process, is occurred during the high speed motion of the activated electron. In the end of the process the electron system is in its normal state. **So we see, that in this case the emission of the 511 keV photon is caused by a self oscillation of the electron in a strong amplitude mode, if the oscillation amplitude reach some threshold.**

It is interesting to investigate the following outcomes of this particular case:

- does the process terminates with emission of two or one 511 keV gamma photon?
- if two gamma photons are emitted, are they orthogonally polarized?

The experiment however is performed only with one detector.

Summary:

- **The $1^3S_1 - 2^3S_1$ transition gives an indirect confirmation, that the proper frequency of the free positron is twice the Compton frequency.**
- **The pumping energy between quantum motions in loops with different velocities is equal to the carrier energy difference multiplied by the pumping efficiency.**

3.17.5 Positron “thermalisation”

In the process, known as a “positron thermalisation”, a thin plate of proper metal, cut at proper crystal plane, is radiated by positive Beta particles (quasiparticle wave). The quasiparticle wave enter into oscillations with a free normal electron of the plate, forming an oscillating system. The CL space inside the sample, however, is different, than the free space (vacuum). Due to the influence of the proton’s fields, and the motion of the formed oscillating system in CL environment with stiffness gra-

dent, the internal positron may come out at much smaller energy of the Beta particle. So a two possibilities may exist in this case:

- the thermalised beam is comprised of particle positrons
- the thermalised beam include both: particle positrons, and quasiparticle waves with reduced energies.

It is more logical to expect the first option, but the second one is not excluded.